Ideal shear banding in metallic glass

J. G. Wang[a,c], H. B. Ke[b], Y. Pan[a], K. C. Chan[d], W. H. Wang[e], J. Eckert[f,g]

[a]School of Materials Science and Engineering, Southeast University, Nanjing 210096, China

[b]China Academy of Engineering Physics, P.O. Box 919-71, Mianyang 621900, Sichuan Province, China

[c]School of Materials Science and Engineering, Anhui University of Technology, Ma'anshan 243002, China

[d]Department of Industrial and Systems Engineering, The Hong Kong Polytechnic University, Hong Kong

[e]Institue of Physics, Chinese Academy of Sciences, Beijing 100190, China

[f]IFW-dresden, Institute for Complex Materials, P. O. Box 270116, D-01171 Dresden, Germany

[g]TU Dresden, Institute of Materials Science, D-01062 Dresden, Germany

Abstract

As the most fundamental deformation mechanism in metallic glasses (MGs), the shear banding has attracted a lot of attention and interest over the years. However, the intrinsic properties of the shear band are affected and even substantially changed by the influence of non-rigid testing machine that cannot be completely removed in real compression tests. In particular, the duration of the shear banding event is prolonged due to the recovery of the stressed compliant frame of testing machine and therefore the temperature rise at the operating shear band is, more or less, underestimated in previous literatures. In this study, we propose a model for the 'ideal' shear banding in metallic glass. The compliance of the testing machine is eliminated, and the intrinsic shear banding process is extracted and investigated. Two important physical parameters, the sliding speed and the temperature of shear band, are calculated and analysed on the basis of the thermo-mechanical coupling. Strain-rate hardening is proposed to compensate thermal softening and stabilise the shear band. The maximum value of the sliding speed is found to be on the order of 10 m/s at least, and the critical temperature at which strain-rate hardening begins to take effect should reach as high as 0.9 T_g (T_g is the glass transition temperature) for a stable shear banding event in metallic glass according to the early experimental data. This model can help to understand and control the shear banding and therefore the deformation in MGs.

Key words: metallic glass; shear banding; temperature rise; thermo-mechanical coupling

1. Introduction

Unlike their crystalline counterparts, metallic glasses (MGs) lack structural defects such as dislocations which can cause strain hardening [1]. It is impossible to spread out the plastic strain in the entire MG specimen if the mechanical tests are conducted well below the glass transition temperature [2,3]. Thin shear band usually develops to accommodate the most plastic strain once the MG yields, insensitive to the strain rate [4,5]. As a result, the process of shear banding plays a vital role in the plastic deformation of MGs. A stable shear band can retard or stop itself after initiating, which avails metallic glass of plastic deformability. An unstable one usually runs away and leads to the brittle fracture. Unfortunately, there is no consensus on the shear banding process so far due to the limited spatiotemporal resolution of the instruments for investigating [5]. Inspired by the river patterns and molten droplets on the fracture surface, one may intuitively think the temperature rises significantly in the shear band [6–8]. Lewandowski and Greer [9] employed a tin coating and estimated that the temperature rise ΔT over 3000 K. However, Wright et al. [10,11] investigated the shear banding event using high frequency strain gauge, piezoelectric load cell as well as video camera, and eventually calculated the ΔT only tens of kelvins, so they concluded that the significant temperature rise results from the final fracture instead of shear banding. This conclusion is supported by some experimental observations using fusible coating method [12,13]. Cheng et al. [14] covered the possibilities of cold and hot shear bands, and they suggested the hot shear band always leads to catastrophic failure of the sample. These early studies took the time spent in the load drop of a serration in the stress–strain curve as the duration of the shear banding event. In fact, measurement of the duration involves the response of testing machine. On one hand, it is extremely difficult to evaluate the effective inertia of the machine-sample system, as claimed in Ref. [14]. On the other hand, the dynamic recovery of the elastic-strained testing machine was not been taken into account in previous works [5,14,15] while the shear banding event is purely dynamic. As a result, the substantial influence and interference from the non-rigid testing machine are not eliminated or understood thoroughly, and the fully intrinsic behaviour of shear banding itself in MGs is therefore still a mystery.

In this work, we present an ‘ideal’ shear banding model in MGs. In our model, the stiffness of testing machine, km, is supposed to be infinitely large, so the absolutely rigid machine will not supply extra energy into the shear band and its influence is absent during the shear banding event [14–17], which makes it possible to investigate the intrinsic properties of the shear band itself. In this sense, the model is called ‘ideal’. Constitutive equations for the thermo-mechanical coupling in the shear banding process are established and solved, and then the solutions are in turn used to describe the shear banding process in MGs. Accordingly, two main physical parameters, i.e. the temperature and the sliding speed of shear band, are obtained and analysed in a quantitative manner. Reasonable ranges for these key physical parameters are

presented and employed to understand and explain the various experimental observations on the deformation behaviours in MGs.

2. The premise for the ideal shear banding model

Figure 1(a) illustrates the fundamental scenario for the ideal shear banding. To avoid confusion and misunderstanding in physics and mathematics, we emphasise several items as follows:

(I) As presented in Figure 1(a), the testing machine is assumed to be perfectly rigid, i.e. $k_m \to \infty$. As a result, there is no need to take account of the influence of the machine in the model any longer.

(II) When the yield stress is reached, the pressing platen stops and keeps still in the following period. This point will be discussed and validated in following text.

(III) Only one single primary shear band is presumed to develop in the plastic deformation of MG. Although multiple secondary shear bands have extensively been observed by scanning electron microscope (SEM), two parts of a deforming MG sample usually slide along a primary single shear band unless they are blocked geometrically, e.g. through touching the pressing platen [18–20]. Therefore, this presumption is quite acceptable in practice.

(IV) There are of course a number of shear banding events as characterised by the serrations in the strain–stress curve for the plastic deformation of MG, but only one event is studied in this paper, because others share the same nature.

(V) The elapsed time of the investigated shear banding event is about $2l/v_l$ ($2l$ is the length of the specimen in Figure 1(a) and is the longitudinal wave speed) in our model. After the first period of $2l/v_l$, our model might not be valid any longer, so it is just applicable during this period. Detailed estimation is given in the Appendix 1.

(VI) A fully developed shear band slides in a simultaneous way rather than propagates in a progressive way. In general, the propagation happens prior to the sliding [5,21]. Direct imaging video confirms that a mature shear band prefers to slide simultaneously [11]. So the simultaneous sliding manner is adopted in this model.

(VII) Free volume creation and annihilation, considered to play an important role in the deformation of metallic glass [2], are not taken into account in our model. This is because the free volume is of importance mainly before the shear band is fully developed [5]. On the other hand, our model only concentrates on the thermo-mechanical coupling for the mature shear band on a macro-scale instead of on an atomic scale.

(VIII) The thickness of an operating shear band, $2h$, as marked in Figure 1(b), is fixed during the shear banding event to simplify the mathematical solution. However, the shear band tends to thicken when the temperature rises significantly at the band [5]. To make up for this deficiency, different hs are taken.

3. The model and the results

3.1 The temperature rise of perturbation

There are a number of physical mechanisms, for instance, free volume generation [2], shear transformation [3], coordinate transformation [22], soft spots [23]and flow unit [24] for the initiation of shear bands, while this paper does not intend to explore any reason why the shear band is initiated. The basic prerequisite of our model is that the shear band already initiates at yield stress. As well known, the formation of a shear band implies yielding of MGs [4,5], which can be identified by the stress drop in the stress–strain curve, i.e. the serration. This drop means that the stress level in shear-band material decreases, and a fraction of elastic energy stored inside the shear-band material is released. According to the law of energy conservation, the released energy must be converted to heat which is absorbed and used to elevate the temperature of the shear-band material itself. The initial temperature rise of perturbation, T_p, is given by

$$T_p = \frac{\alpha \sigma_y^2}{2E\rho c} \qquad (1)$$

in which σ_y is the yield stress, E the Young's modulus, ρ the density and c the specific heat. α is a dimensionless factor concerning two physical facts. One is how much fraction of σ_y the stress drop accounts for at the beginning of yielding. The other one is how much fraction of the released elastic energy is used to heat the shear-band material, since some energy is consumed outside the shear band. Although these two aspects are still unclear, α must have a value of less than unit but greater than zero, i.e. $0 < \alpha < 1$, and $\alpha = 0.1$ adopted in this study. It should be noted that the model is not sensitive to the value of α [See supplementary material for the influence of values of α in Equation (1) and a and b in Equation (5)]. As a consequence, when the time $t = 0$ s, the temperature of the shear band is

$$T_i = T_R + T_p \qquad (2)$$

in which T_R =300 K is the room temperature.

3.2 The temperature dependence of strength

In general, the strength σ_s of a certain material depends on temperature T, strain ε, and strain rate $\dot{\varepsilon}$ as [25-26]

$$\sigma_s = \sigma_s(\varepsilon, \dot{\varepsilon}, T) \qquad (3).$$

Although strain softening [27] and strain hardening [28] are both proposed in monolithic MGs, the structural reasons for them are under controversy in the community [5]. Taking account of the geometrical effect, Han *et al*. [18] found that the strength of a Zr-based MG is basically invariant at a quasi-static rate (10^{-4} s^{-1}), regardless of the strain. As a result, Equation (3) can be modified in metallic glass:

$$\sigma_s = \sigma_s(\dot{\varepsilon}, T) \qquad (4)$$

Unfortunately, there still lacks a simple and applicable analytical formulation for Equation (4) on the macroscopic scale, though the atomic scale models considering T and $\dot{\varepsilon}$ for the deformation in MGs have been developed, e.g. the free volume model and the shear transformation zone model [4-5]. Since the strength of MG is insensitive to the strain rate when $T<0.9T_g$ (T_g is the glass transition temperature), the temperature dependence of the strength of MGs is found to have a linear form as follows [29]:

$$\sigma_s = (a - \frac{bT}{T_g})E \qquad (5)$$

where both a and b are fitting constants.

3.3 The motion of the shear band

Once the flow stress in shear band decreases below σ_y, the sample will slide along the band due to the driving force from the surrounding elastic matrix at a little higher stress level. However, the shear plane as marked by the dotted line in Figure 1(b) holds still because the two parts separated by the shear band move symmetrically towards each other. We take the upper part of the specimen in Figure 1(a) as the object of study. As mentioned above, because the shear banding process goes dynamically, the inertia of every segments of the specimen must be considered. Their motion are governed by the wave equation [26]

$$\frac{\partial^2 u}{\partial t^2} = {v_l}^2 \frac{\partial^2 u}{\partial y^2} \qquad (0 \le y \le l) \qquad (6)$$

in which $u(y,t)$ is the displacement at position y and at time t, v_l is the longitudinal wave speed, and l the half length of the sample. When $t = 0$, it has

$$u\big|_{t=0} = -\frac{\sigma_y}{E} y \qquad (7a)$$

$$\left.\frac{\partial u}{\partial t}\right|_{t=0} = 0 \qquad (7b)$$

The minus in Equation (7a) indicates the compressive stress. Equation (7b) describes that the sample is motionless in the beginning, corresponding to the statement (II). The boundary conditions are given by

$$u\big|_{y=0} = 0 \qquad (8a)$$

$$\left.\frac{\partial u}{\partial y}\right|_{y=l} = -\frac{\sigma_s}{E} \qquad (8b)$$

Equation (8a) also corresponds to the statement (II), and σ_s in Equation (8b) is formulated in Equation (5) and depends on the temperature, while σ_y is a constant in Equations (1) and (7a). To solve Equation (6) under the conditions of Equations (7) and (8), T with time at the centre of the shear band is needed in Equation (5).

3.4 The temperature rise of the shear band

Since the elastic energy stored in the sample is released and transferred into the shear band and converted to heat, the temperature of the shear-band material must increase. The shear band is so thin that it can be considered to be uniform along the thickness direction. As such, the heating power density within the shear band is

$$\omega = \frac{\beta \tau v}{h} \qquad (9)$$

in which $\tau = \frac{\sigma_s}{2}$ is the shear stress in the shear plane, $v = \sqrt{2}\left.\frac{\partial u}{\partial t}\right|_{y=l}$ is the sliding speed of the shear band when the shear angle θ=45^o in Figure 1(a) is taken [30], h is the half thickness of the shear band (see details in Figure 1(b)). β is a dimensionless factor usually taken as 0.9 [25] because a small fraction of the elastic energy is consumed in terms of acoustic and light emission and sometimes by the change of atomic configuration. Now, we have the evolution of temperature inside and around the shear band with time (because of the spatial symmetry about the shear plane x = 0 as shown in Figure 1(b), only the x positive direction is considered) [31],

$$\frac{\partial T}{\partial t} = \kappa \frac{\partial^2 T}{\partial x^2} + \frac{\omega}{\rho c} \qquad (x < h) \qquad (10a)$$

$$\frac{\partial T}{\partial t} = \kappa \frac{\partial^2 T}{\partial x^2} \qquad (x > h) \qquad (10b)$$

where κ is the thermal diffusivity. Obviously, it has the initial conditions (t =0 s) as follows

$$T = T_i \qquad (x<h) \qquad (11a)$$

$$T = T_R \qquad (x>h) \qquad (11b)$$

and the boundary conditions given by

$$\left.\frac{\partial T}{\partial x}\right|_{x=0} = 0 \qquad (12a)$$

$$T\big|_{x\to\infty} = T_R \qquad (12b).$$

Given the symmetry around the shear plane x = 0, there is no temperature difference between the two sides just across the shear plane, so Equation (12a) holds. Equation (12b) means that the temperature at a position far enough away from the shear band is not affected and keeps the original value.

Apparently, it is impossible to find analytical solutions to Equations (6) and (10) which actually are thermo-mechanically coupled via Equation (9). We solve them numerically using the physical parameters of Vitreloy1 [22,32-33]. The values for these parameters are listed in Table I. a=0.02468 and b=0.0106 in Equation (5) are adopted according to Ref. [30] and altered

slightly to insure σ_s=σ_y=1.86 GPa at room temperature.

It should be noted that the boundary condition Equation (12b) is not achievable in practice because of the infinity of x. Actually, it can be approximated in two extreme ways:

$$T\big|_{x=x_b} = T_R \qquad (13a)$$

$$\left.\frac{\partial T}{\partial x}\right|_{x=x_b} = 0 \qquad (13b)$$

where x_b>>h. Equation (13a) means the temperature at x=x_b keeps constant T_R, implying no heat accumulation there, while Equation (13b) implies no heat diffusion or complete heat accumulation. Obviously, Equation (12b) lies in between. In fact, if h is taken to 0.01~1.00 μm according to the previous studies [5], it is found that the boundary conditions (13a) and (13b) will give the same results when x_b = 20 μm.

3.5 No consideration of the influence of strain rate on the strength

Figure 2 shows the sliding speed v and the temperature T of the shear band with time t before T reaches T_g for a Vitreloy1 specimen of l = 2 mm, and the effect of the strain rate on the strength is neglected. v vs. t is plotted in Figure 2(a) with h = 0.01 μm (red curve), 0.10 μm (green curve) and 1.00 μm (blue curve). One can see that v increases up to 38.6 m/s within a very short time. It is about four orders of magnitude higher than that (~10^{-3} m/s) suggested by Cheng *et al*. [14], but it is still only about one hundredth of the sound wave speed [32,34]. Figure 2(b) shows the temperature evolution with time at the centre of the shear band. Clearly, it takes a longer time for h = 0.01 μm than for h = 1.00 μm to reach T_g. It has an extremely similar profile to that in Figure 2(a). Taking those values for h = 0.10 μm, Figure 2(c) shows their match and coincidence. Obviously, the temperature and the sliding speed are physically coupled, as both cause and effect.

The temperature dependence of strength, i.e. Equation (5), is achieved using bulk specimens which are heated overall in Ref. [30]. It is well known that the shear band is a thin layer, just a small fraction of the specimen, as illustrated in Figure 1(b). As a result, Equation (5) may not hold true any longer because a thin layer of viscous material usually can resist larger flow shear stress than the bulk [35]. Unfortunately, there is no experimental data on the shear behaviour of the thin layer of metallic glass, thus a compromise formula is taken here. The slope value in Equation (5) is reduced by half, i.e. b = 0.0053, and a = 0.02213 is therefore taken to insure σ_s = 1.86 GPa at 300 K (hereinafter a and b remain the same values). Figure 3 shows the sliding speed and the temperature of shear band with time in a 2 mm long vitreloy1 specimen under the updated temperature dependence of strength. Apparently, the evolution of the sliding speed is closely related to that of the temperature at the shear band, no matter how

thick the shear band is. On the other hand, the increase rates of both v and T decrease with the thickness of the shear band, similar to the presented in Figure 2. This demonstrates that the thermo-mechanical coupling in the shear banding event is not sensitive to the specific form of Equation (5), provided that the strength of the MG decreases with temperature, i.e. $b > 0$ [See supplementary material for the influence of values of α in Equation (1) and a and b in Equation (5)].

3.6 The influence of strain rate on the strength

The influence of the strain rate is becoming more and more significant when the temperature increases, and cannot be neglected when T approaches T_g [36]. In general, the strength of materials increases with increasing strain rate. In other words, the strain rate sensitivity is usually positive if the temperature effect is also considered [26,37]. As shown in Figure 1, the specimen is sheared in mode II [1]. Therefore, only the shear stress component τ is affected by the shear strain rate, whereas the normal stress component σ_n is not. As a result, Equation (5) is complemented by [25]

$$\sigma_s = \tau(\frac{\dot{\gamma}}{\dot{\gamma}_r})^m + \sigma_n \qquad (T>T_{cr}) \qquad (14)$$

where $\tau = \sigma_n = \frac{1}{2}\sigma_s$, $\dot{\gamma}$ and m are the shear strain rate and the shear strain rate sensitivity, respectively, $\dot{\gamma}_r$ is the reference shear strain rate below which the flow stress is independent of the strain rate, and T_{cr} is the critical temperature beyond which Equation (5) is replaced by Equation (14). For different kinds of crystalline metals and alloys, m is similar, and on the magnitude order of 10^{-2} [25]. Pan *et al.* [38] measured Pd-, Pt-, Zr-, Cu- and Ni-based MGs using nanoindentation and found that their m values range from 6.7×10^{-3} to 2.1×10^{-2}. Then the value of m is also set on the order of 10^{-2} in the present study. Since there is no strain hardening in MGs as discussed in Section 3.2, the shear bands cannot slide in a stable way due to the thermal softening if m is negative, i.e. strain-rate softening, as suggested in Ref. [38]. This is inconsistent with some previous experimental works in which shear bands are found stable [8,10,11,17,19]. Therefore, a positive m should be logically accepted. In addition, is taken as10^{-3} s^{-1} and kept constant in this paper [4].

We now consider the influence of the shear strain rate. The temperature dependence of the strength is formulated by Equation (5) when $T<T_g$ and by Equation (14) when $T>T_g$ (i.e. $T_{cr}=T_g$). Moreover, once the strength calculated by Equation (14) is larger than σ_y due to the very high, the other shear band will develop elsewhere because of this strain-rate hardening, which is in contradiction with the statement (III). Therefore, if the calculated occurs, we set in Equation (14) in the numerical calculation. The plots of v and T vs. t are combined in Figure 4(a) with m = 0.01 and h = 0.10 μm. Obviously, the profile shown in lower left corner enclosed by the green-

dotted rectangle in Figure 4(a) is just the median one in Figure 3. After the temperature reaches T_g (623 K) at t = 110 ns, v begins to drop steeply because Equation (5) is replaced by Equation (14) and the strain-rate hardening begins to take effect. From t = 120 ns to 270 ns, the sliding of the shear band decelerates slightly, while the temperature remains T_g. In 300 ns as labelled by Δt, v increases rapidly, and so does T. At t = 500 ns, v seems to approach a saturation value in excess of 120 m/s, and T rises close to 2500 K. The whole shear banding process comes to the end at ~800 ns, which indicates that the displacement of the pressing platen will be on the order of 10^{-12} m if the movement of the pressing platen is considered (the strain rate is ~10^{-3} s^{-1} and l is ~10^{-3} m). Obviously, this displacement is negligible compared with the sliding displacement of shear band (~10^{-6} m), so the statement (II) above can hold. Given that the liquidus temperature of vitreloy1 is 996 K, the shear-band material must be melted. More important, one can infer that the high sliding speed of ~120 m/s makes the shear banding unstable and will lead to the failure or fracture of specimen. However, if the specimen is shorter, the shear banding event will be complete within Δt (~300 ns) and therefore it should be stable in that it has not enough time to run away. Taking l = 0.5 mm in Figure 1(a), Figure 4(b) shows that the sliding speed reaches the peak value at t = 110 ns, identical to the profile enclosed in the lower left corner in Figure 4(a). Then it decreases till the end of the shear banding event, while T constantly remains at the glass transition temperature. It demonstrates that the shear banding in a shorter specimen is stable indeed. This is essentially in agreement with the results by Cheng *et al*. [14], Han *et al*. [15], and Yang *et al*. [16] who all suggest that a shorter specimen is more likely to be sheared in a stable way.

As aforementioned, the strain-rate sensitivity m in Equation (14) can be as large as 0.02 [38]. The numerical solutions for v and T with m = 0.02 (other parameters are the same as those for Figure 4(a)) are plotted in Figure 5(a). One can see that the curves of v and T against t are very similar to those in Figure 4(b), though their durations are different due to the different ls. As expected, the increment of m is helpful to stabilise the shear banding. In fact, a positive m means the strain-rate hardening. A larger m can therefore hinder or even prevent the runaway sliding of the shear band. On the other hand, experimental observation confirms that the effect of the strain rate on the strength of MGs actually shows up at 0.9Tg [36,39]. Now we let T_{cr} = 0.9 T_g in Equation (14) and keep other parameters the same as those for Figure 4(a), and then find v and T against t by the numerical method. Figure 5(b) presents their profiles, significantly different from those in Figure 4(a). In addition, the peak value of the sliding speed is lowered in comparison with that in Figure 5(a), and the temperature never exceeds 0.9 T_g (i.e. T_{cr}) during the whole shear banding process. As such, a smaller T_{cr} actually plays a similar role to a larger m in stabilising the shear banding.

4. Discussions

4.1 The thermo-mechanical coupling

In MGs, it has been studied for a long time that the sliding of shear band can result in a temperature rise, more or less, at the shear band [5]. Although some attention is paid to correlation between the yield and the shear band formation in metallic glass [40], the thermo-mechanical coupling during the sliding of the shear band is not described enough clearly or deeply. Our results duly show this coupling in which the sliding is facilitated by the temperature rise softening the shear-band material. In Figures 2 and 3, it is hard to tell which one (v or T) is the cause or the effect because they increase with time in parallel. In Figure 4(a), the temperature does not increase monotonically, but reaches a plateau in the intermediate period instead. This plateau is due to the reduction of sliding speed which results from the strain-rate hardening formulated in Equation (14). One can imagine that the temperature difference between inside the shear band and the surrounding matrix is lessened during the plateau. According to the Fick's first law, the diffusion flux of heat is therefore lowered due to the smaller temperature difference [31]. Once the heat diffusion flux decreases less than the supply rate of energy, the temperature inside the shear band increases again dramatically because of the net heat accumulation, as illustrated in latter part (i.e. $t > 300$ ns) of Figure 4(a). In contrast, an insignificant temperature rise will also be possible if T_{cr} drops down close to room temperature and the methodology in Figure 5 is followed.

4.2 The shear strain rate sensitivity and the critical temperature

Unlike the length (i.e. $2l$ in Figure 1(a)) of a specimen which can be measured precisely, neither the critical temperature T_{cr} nor the strain-rate sensitivity m can be obtained easily. m of course varies in different glassy alloys with different chemical compositions. For instance, the m for $Pd_{40}Ni_{40}P_{20}$ is 6.7×10^{-3}, while that for $Zr_{44}Cu_{44}Al_6Ag_6$ is 2.1×10^{-2} [38]. On the other hand, when the glass-forming liquid is quenched into a glassy solid, it can be trapped in one of numerous possible megabasins in the energy landscape [41]. As a result, m of a MG with a certain composition is not a constant due to the slight difference of atomic configuration. At the same time, m is also affected by the instant temperature and strain rate during the shear banding event. In comparison, T_{cr} is relatively easy to determine according to the experimental data, usually no less than $0.9T_g$. Nevertheless, T_g can be shifted by the cooling rate [42-43] and thermal history [43-44]. In other words, T_{cr} is not simply fixed either. As such, specimens of the same composition and geometry can show varied stability of shear banding under the same loading conditions of strain rate and test machine stiffness, which is well described by the Weibull distribution [41]. One can easily understand this kind of randomness in Figures 4 and

5. On the contrary, previous literatures only paid attention to the length and diameter of the specimen and the test machine stiffness, and did not take account of the intrinsic properties, i.e. m and T_{cr}, of the alloy, so they are unable to explain the scattering stabilities of shear banding in MGs [14–17].

4.3 The temperature rise, significant or not

In comparison, the duration of the shear banding event is measured on the order of 10^{-4}~10^{-3} s by high frequency video camera (10^4~10^5 Hz) and load cell (~10^6 Hz) [10-11], more than three orders of magnitude longer than that (~10^{-7} s) proposed by our analysis. According to the spacing between the striations on the shear plane, early studies give 10^{-3} m/s as the maximum sliding speed of shear band [10-11,14,17,19], about four orders of magnitude smaller than our result (~10 m/s). In fact, early analyses and calculations have improperly taken into account the inertia of the testing machine just since the initiation of the shear band [14–17,45]. At just the beginning of the shear banding event, the testing machine and even the end of the specimen actually do not 'know' that the shear band is initiated, and they will receive the message after a period of ~l/v (l is illustrated in Figure 1(a)). Obviously, this period is so short (10^{-7} s) that it is already complete when the first image is captured by a high frequency camera (10^5 Hz, i.e. time interval of 10^{-5} s). In a real compression test using a non-rigid testing machine, the shear event is prolonged because of the recovery of the loaded compliant machine which will push the specimen to continue to move for a while after this short period [14]. The movement is accomplished slowly owing to the large inertia of the test machine. Consequently, the temperature rise at the shear band is calculated to be insignificant based on the prolonged duration of the shear banding event. Nevertheless, at least two different groups applied tin coating onto the surface of MG, and then found the coating unfused at shear bands in deformed MG [12-13], so they suggest that the temperature rise at the shear band is small. Logically, it must be accepted that the fused coating definitely indicates a significant temperature rise (say, ΔT_1), but unfused coating material never means insignificant temperature rise (say, ΔT_2). Despite $\Delta T_1 > \Delta T_2$, $\Delta T_2 + T_R$ must be no less than T_{cr} (>$0.9T_g$) in Equation (12) for a stable shear banding event. If T_{cr} is higher than the melting point of the tin coating, will the coating certainly be melted? There are two factors needed to consider. (i) There is an interface between the coating and the substrate (i.e. MG specimen), so the heat conduction may be delayed or blocked by this interface to a certain degree. If the interface is not well connected, the heat cannot be accumulated soon enough to elevate the temperature of the coating material because the heat also diffuses out to the air from the surface of the coating [25]. (ii) If the coating is too thick, a lot of heat is required to render it hot enough to melt. The thickness of the coating is usually tens of nanometres [9,11-12], and it is proposed that several nanometres will be more sensitive. As a result, if $\Delta T_2 + T_R$ is just only a little higher than the liquidus temperature of the coating,

the coating probably cannot melt. For a runaway shear band as described in Figure 4(a), the temperature at shear band can be over 2000 K, so the coating tin can melt for sure. Sometimes, no molten droplets but only striations can be found on the shear plane of the sheared MG specimen, so it is claimed that the shear band cannot be hot [14,17,19]. In fact, the absence of molten droplet only implies that the temperature at the shear band is below the liquidus temperature of the investigated MG, but it never means the shear band is cold. As analysed in our model, the temperature at a stable shear band is as high as T_{cr} at least. And T_{cr} is no less than $0.9T_g$ according to the previous experimental studies. If the temperature at the shear band cannot reach 0.9 T_g, cracking would likely take place prior to shear banding in MGs. In brittle MGs like Mg- [46-47] and Fe-based [48] glassy alloys which often preferentially fail by cracking rather than by shear banding, no any striation or molten droplet can be observed on the fracture surface, indicating that the temperature rise is negligible indeed. On the other hand, if the test is conducted at cryogenic temperature and the maximum temperature at the shear band cannot arrive at 0.9 T_g despite a significant temperature rise, then the strain-rate hardening (i.e. Equation 14) will not take effect and nothing can stabilise the shear band, so the metallic glass will fracture in a brittle manner and the molten droplets disappear. This has been witnessed and well verified by Jiang *et al.* recently [49].

5. Conclusion

We present an ideal shear banding model in metallic glass which can get rid of the influence of the testing machine. It is found that the flow stress of the shear-band material depends on its temperature as well as the sliding speed of the shear band. A high temperature lowers the shear resistance in the shear band and therefore facilitates the sliding which in turn supplies the energy into the band to elevate the temperature further. Based on this thermo-mechanical coupling, the temperature and the sliding speed of the shear band have been calculated by numerical method. The strain-rate hardening is needed to compensate the thermal softening to make the shear band slide in a stable way. If the compensation is not strong enough, the shear banding will suffer a dynamic instability leading to the failure of the specimen. Since the capacity for compensating depends not only on the atomic configuration in energy landscape but also on the instant dynamic process in test, the stability of shear banding in the MGs cannot simply be described by the geometry of specimen and the stiffness of the testing machine. Besides, it is proposed that the shear banding must result in a significant temperature rise, otherwise cracking may take place and cause the catastrophic fracture, like the case in brittle Fe- and Mg-based MGs. Our modelling, calculation and analysis present the intrinsic behaviour of the shear banding in MGs. These findings might help to better understand, describe and take advantage of the shear banding process in MGs.

Acknowledgements

This work was financially supported by NSF of China [grant number 51201001] and the China Postdoctoral Science Foundation [grant number 2014M561550]. J. Eckert acknowledges the supports from the German Science Foundation (DFG) under the Leibniz Programme [grant number EC 111/26-1] and the European Research Council under the ERC Advanced Grant INTELHYB [grant number ERC-2013-ADG-340025].

Appendix

As shown in Figure A1(A), an l long rod with one end fixed on the left is stressed by $\Delta\sigma$ on the right end. The full and dashed rectangles illustrate the sample before and after the remove of the $\Delta\sigma$, respectively. If the $\Delta\sigma$ is suddenly removed, the displacement of the free right end as a function of time is [26]

$$u = -\frac{8l\Delta\sigma}{E\pi^2}\sum_{n=0}^{\infty}\frac{1}{(2n+1)^2}\cos\frac{(2n+1)\pi vt}{2l} \qquad \text{(A1)}$$

where E is Young's modulus and v is the longitudinal wave speed. Therefore, the speed of the free end is

$$\dot{u} = \frac{4v\Delta\sigma}{E\pi}\sum_{n=0}^{\infty}\frac{1}{(2n+1)}\sin\frac{(2\mathrm{n}+1)\pi vt}{2l} \qquad \text{(A2)}$$

Figures A1(B) and (C) graphically show u and $\dot{u}$ with time, respectively. Obviously, they are both periodic functions with , $u_m = \frac{l\Delta\sigma}{E}$, $\dot{u}_m = \frac{v\Delta\sigma}{E}$, and $\tau_0 = \frac{2l}{v}$ (τ_0 is the half period). During the first half period, the end, touching the pressing platen in Figure 1(a) but unfixed, of the specimen is equivalent to a fixed end, because it doesn't move away. Once it enters the second half period, the free right end in Figure A will come back. If the left end is not really fixed, the specimen cannot withdraw its free right end to recover. This is the case in Figure 1(a) when the shear band is compared to the free end in Figure A1(A). As a result, the shear b and suddenly stops sliding at the end of the first half period. It means the duration of a shear banding event is about $2l/v_l$ in our model.

References

[1] T.H. Courtney, Mechanical Behavior of Materials. McGraw-Hill Company, Inc. 2000.

[2] F. Spaepen, A microscopic mechanism for steady state inhomogeneous flow in metallic glasses, Acta Metall. 25 (1977) 407-415.

[3] A.S. Argon, Plastic deformation in metallic glasses. Acta Metall. 27 (1979) 47-58.

[4] C.A. Schuh, T.C. Hufnagel, U. Ramamurty, Mechanical behavior of amorphous alloys, Acta Mater. 55 (2007) 4067-4109.

[5] A.L. Greer, Y.Q. Cheng, E. Ma, Shear bands in metallic glasses, Mater. Sci. Eng. R 74 (2013) 71-132.

[6] C.T. Liu, L. Heatherly, D.S. Easton, C.A. Carmichael, J.H. Schneibel, C.H. Chen, J.L. Wright, M.H. Yoo, J.A. Horton, A. Inoue, Test environments and mechanical properties of Zr-base bulk amorphous alloys, Metall. Mater. Trans. A 29A (1998) 1811-1820.

[7] F. Spaepen, Must shear band be hot? Nature Mater. 5 (2006) 7-8.

[8] K. Georgarakis, M. Aljerf, Y. Li, A. LeMoulec, F. Charlot, A.R. Yavari, K. Chornokhvostenko, E. Tabachnikova, G.A. Evangelakis, D.B. Miracle, A.L. Greer, T. Zhang, Shear band melting and serrated flow in metallic glasses, Appl. Phys. Lett. 93 (2008) 031907.

[9] J.J. Lewandowski, A.L. Greer, Temperature rise at shear bands in metallic glasses, Nature Mater. 5 (2006) 15-18.

[10] W.J. Wright, M.W. Samale, T.C. Hufnagel, M.M. LeBlanc, J.N. Florando, Studies of shear band velocity using spatially and temporally resolved measurements of strain during quasistatic compression of a bulk metallic glass, Acta Mater.57 (2009) 4639-4648.

[11] W.J. Wright, R.R. Byer, X.J. Gu, High–speed imaging of a bulk metallic glass during uniaxial compression, Appl. Phys.Lett. 102 (2013) 241920.

[12] S.V. Ketov, D.V. Louzguine-Luzgin, Localized shear deformation and softening of bulk metallic glass: stress or temperature driven? Sci. Rep. 3, 2798; DOI:10.1038/srep02798 (2013).

[13] S.K. Slaughter, F.Kertis, E. Deda, X. Gu, W.J. Wright, T.C. Hufnagel, Shear bands in metallic glasses are not necessarily hot, APL Mater. 2 (2014) 096110.

[14] Y.Q. Cheng, Z. Han, Y.Li, E. Ma, Cold versus hot shear banding in bulk metallic glass, Phys. Rev. B 80 (2009) 134115.

[15] Z. Han, W.F. Wu, Y.Li, Y.J. Wei, H.J. Gao, An instability index of shear band for plasticity in metallic glasses, Acta Mater. 57 (2009) 1367-1372.

[16] Y. Yang, J.C. Ye, J. Lu, P.K. Liaw, C.T. Liu, Characteristic length scales governing plasticity/brittleness of bulk metallic glasses at ambient temperature, Appl. Phys. Lett. 88 (2010) 221911.

[17] B.A. Sun, S. Pauly, J. Tan, M. Stoica, W.H. Wang, U. Kühn, J. Eckert, Serrated flow and stick-slip deformation dynamics in the presence of shear-band interactions for a Zr-based metallic glass, Acta Mater. 60 (2012) 4160-4171.

[18] Z. Han, H. Yang, W.F. Wu, Y. Li, Invariant critical stress for shear banding in a bulk metallic glass, Appl. Phys. Lett. 93 (2008) 231912.

[19] S.X. Song, H. Bei, J. Wadsworth, T.G. Nieh, Flow serration in a Zr-based bulk metallic glass in compression at low strain rates, Intermetallics 16 (2008) 813-818.

[20] J.G. Wang, K.C. Chan, J.C. Fan, L. Xia, G. Wang, W.H. Wang, Buckling of metallic glass bars, J. Non-Cryst. Solids 387 (2014) 1-5.

[21] R.T. Qu, Z.Q. Liu, G. Wang, Z.F. Zhang, Progressive shear band propagation in metallic glasses under compression, Acta Mater. 91 (2015) 19–33

[22] W.L. Johnson, K. Samwer, A universal criterion for plastic yielding of metallic glasses with a $(T/T_g)^{2/3}$ temperature dependence, Phys. Rev. Lett. 95 (2005) 195501.

[23] J. Ding, S. Patinet, M.L. Falk, Y. Cheng, E. Ma, Soft spots and their structural signature in a metallic glass, Proc. Nat. Acad. Sci. 111 (2014) 14052-14056.

[24] Z. Lu, W. Jiao, W.H. Wang, H.Y. Bai, Flow unit perspective on room temperature homogeneous plastic deformation in metallic glasses, Phys. Rev. Lett. 113 (2014) 045501.

[25] Y. Bai, B. Dodd, Adiabatic Shear Localization: Occurrence, Theories, and Applications (Pergamon, Oxford, 1992).
[26] M.A. Meyers, Dynamic Behavior of Materials, (John Wiley & Sons, Inc., 1994).
[27] H. Bei, S. Xie, E.P. George, Softening caused by profuse shear banding in a bulk metallic glass, Phys. Rev. Lett. 96 (2006) 105503.
[28] J. Das, M.B. Tang, K.B. Kim, R. Theissmann, F. Baier, W.H. Wang, J. Eckert, "Work-hardenable" ductile bulk metallic glass, Phys. Rev. Lett. 94 (2005) 205501.
[29] H. Li, C. Fan, K. Tao, H. Choo, P.K. Liaw, Compressive behavior of a Zr-based metallic glass at cryogenic temperatures, Adv. Mater. 18 (2006) 752-754.
[30] Z.F. Zhang, G. He, J. Eckert, L. Schultz, Fracture mechanisms in bulk metallic glassy materials, Phys. Rev. Lett. 91 (2003) 045505.
[31] H.S. Carslaw, J.C. Jaeger, Conduction of Heat in Solids (Oxford University Press, London, 1959), 2nd, Chapter 2.
[32] W.H. Wang, The elastic properties, elastic models and elastic perspectives of metallic glasses, Prog. Mater. Sci. 57 (2012) 487-656.
[33] M. Yamasaki, S. Kagao, Y. Kawamura, K. Yoshimura, Thermal diffusivity and conductivity of supercooled liquid in $Zr_{41}Ti_{14}Cu_{12}Ni_{10}Be_{23}$ metallic glass, Appl. Phys. Lett. 84 (2004) 4653-4655.
[34] M. Zhao, M. Li, Y.F. Zheng, Assessing the shear band velocity in metallic glasses using a coupled thermo-mechanical model, Philos. Mag. Lett. 91 (2011) 705-712.
[35] J.N. Israelachvili, P.M. Mcguiggan, A.M. Homola, Dynamic properties of molecularly thin liquid films, Science 240 (1988) 189-191.
[36] J. Lu, G. Ravichandran, W. L. Johnson, Deformation behavior of the $Zr_{41.2}Ti_{13.8}Cu_{12.5}Ni_{10}Be_{22.5}$ bulk metallic glass over a wide range of strain-rates and temperatures, Acta Mater. 51 (2003) 3429-3443.
[37] A. Bhattacharyya, G. Singh, K.E. Prasad, R. Narasimhan, U. Ramamurty, On the strain rate sensitivity of plastic flow in metallic glasses, Mat. Sci. Eng.: A. 625 (2015) 245–251.
[38] D. Pan, A. Inoue, T. Sakurai, M.W. Chen, Experimental characterization of shear transformation zones for plastic flow of bulk metallic glasses, Proc. Nat. Acad. Sci. 105 (2008) 14769-14772.
[39] W. L. Johnson, J. Lu, M. D. Demetriou, Deformation and flow in bulk metallic glasses and deeply undercooled glass forming liquids-a self consistent dynamic free volume model, Intermetallics 10 (2002) 1039-1046.
[40] F. Shimizu, S. Ogata, J. Li, Yield point of metallic glass, Acta Mater. 54 (2006) 4293–4298.
[41] H. B. Yu, W. H. Wang, J. L. Zhang, C. H. Shek, H. Y. Bai, Statistic analysis of the mechanical behavior of bulk metallic glasses, Adv. Eng. Mater. 11 (2009) 370-373.
[42] J. Schroers, A. Masuhr, W.L. Johnson, R. Busch,Pronounced asymmetry in the crystallization behavior during constant heating and coolingof a bulk metallic glass-forming liquid,Phys. Rev. B 60 (1999) 11855.
[43] W.L. Johnson, G. Kaltenboeck, M.D. Demetriou, J.P. Schramm, X. Liu, K. Samwer, C.P. Kim, D.C. Hofmann, Beating crystallization in glass-forming metals by millisecond heating and processing, Science 332 (2011) 828-833.
[44] K.J. Dawson, L. Zhu, L. Yu, M.D. Ediger, Anisotropic structure and transformation kinetics of vapor-deposited indomethacin glasses, J. Phys. Chem. B 115 (2011) 455-463.
[45] D. Klaumünzer, A. Lazarev, R. Maaß, F.H. Dalla Torre, A. Vinogradov, J.F. Löffler, Probing shear-band initiation in metallic glasses, Physical Review Letters. 107 (2011), pp. 185502.
[46] X.K. Xi, D.Q. Zhao, M.X. Pan, W.H. Wang, Y. Wu, J.J. Lewandowski, Fracture of brittle metallic glasses: brittleness or plasticity, Phys. Rev. Lett. 94 (2005) 125510.
[47] G. Wang, D.Q. Zhao, H.Y. Bai, M.X. Pan, A.L. Xia, B.S. Han, X.K. Xi, Y. Wu, W.H. Wang, Nanoscale periodic morphologies on the fracture surface of brittle metallic glasses, Phys. Rev. Lett. 98 (2007) 235501.
[48] Q.J. Chen, J. Shen, D.L. Zhang, H.B. Fan, J.F. Sun, Mechanical performance and fracture behavior of $Fe_{41}Co_7Cr_{15}Mo_{14}Y_2C_{15}B_6$ bulk metallic glass, J. Mater. Res. 22 (2007) 358-363.
[49] M.Q. Jiang, G. Wilde, J.H. Chen, C.B. Qu, S.Y. Fu, F. Jiang, L.H. Dai, Cryogenic-temperature-

induced transition from shear to dilatational failure in metallic glasses, Acta Mater. 77 (2014) 248-257.

Figure captions

Figure 1. Schematic illustration of the shear band in metallic glass under compression. (a) A 2l long MG specimen compressed by a perfectly rigid machine and a primary shear band developing with a shear angle θ=45^o in the middle of the specimen. (b) An enlarged view of the circled region in (a) illustrating the thickness of the shear band.

Figure 2. Thermo-mechanical coupling in a vitreloy1 specimen with a length of 4 mm, three different shear-band thicknesses and the temperature dependence of strength formulated by Equation (5) where a=0.02468 and b=0.0106. (a) Profile of the sliding speed of a shear band with time and (b) for that of the temperature at the shear band with time. (c) A superimposed profile showing the coincidence of the sliding speed and the temperature of the shear band with h=0.10 μm.

Figure 3. Thermo-mechanical coupling in the other 4 mm long vitreloy1 specimen with the temperature dependence of strength formulated by Equation (5) where a=0.02213 and b=0.0053. Obviously, the profiles are extremely similar to those in Figure 2, indicating that the coupling is not sensitive to the specific form of Equation (5).

Figure 4. The thermo-mechanical coupling in a vitreloy1 specimen under the consideration of strain-rate hardening with m=0.01 and T_{cr}=T_g in Equation (14). (a) The half length of the specimen is 2 mm and the shear banding is unstable. (b) The shear banding is stable due to the shorter length of the specimen, i.e. 2l=1 mm.

Figure 5. A comparison with Figure 4. (a) m=0.02 and T_{cr}=T_g. (b) m=0.01 and T_{cr}=0.9T_g. In both cases, the shear banding is stable and the dynamic stability of shear banding is sensitive to m and Tcr in Equation (14).

Figure in Appendix: Dynamic behaviour of a stressed rod with its left end fixed. (A) Sketch of the recovery of the stressed rod. Full and dashed rectangles illustrate the sample before and after the removal of stress, respectively. (B) The displacement of the right free end of the recovering rod with time and (C) the speed of that.

Tables

Table 1. The data for the physical parameters of vitreloy1. σ_y yield stress, E Young's modulus, ρ density, c specific heat, κ thermal diffusivity, v_l longitudinal wave speed and T_g glass transition temperature [22,31-32]. It should be noted that c = 520 J kg^{-1} K^{-1}, $\kappa = 3.5 \times 10^{-6}$ m^{-2} s and v_l = 5000 m s^{-1}are adopted in the numerical calculation.

σ_y (GPa)	E (GPa)	ρ (kg m^{-3})	c (J kg^{-1}K^{-1})	κ (10^{-6} m^{-2} s)	v (m s^{-1})	T_g (K)
1.86	95	5,900	380~520	2.0~3.5	5,174	623

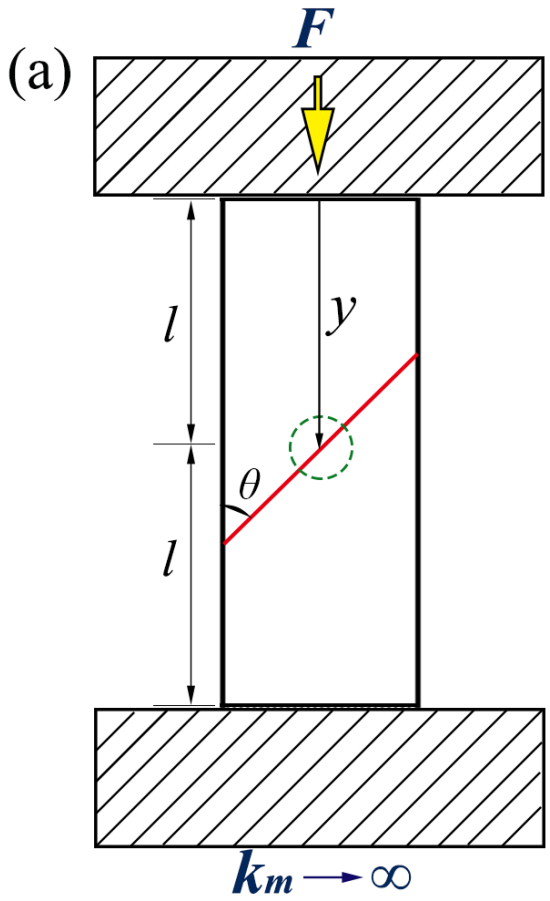

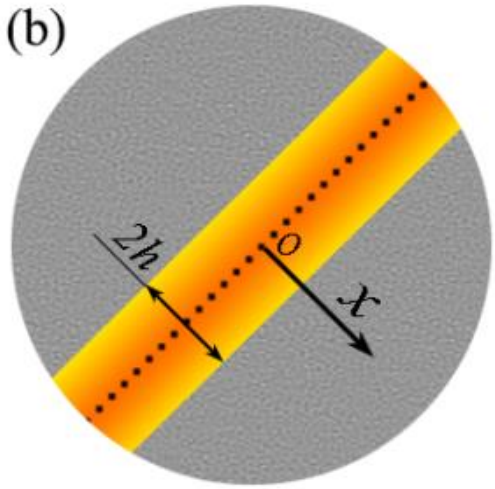

Figure 1 J. G. Wang *et al*

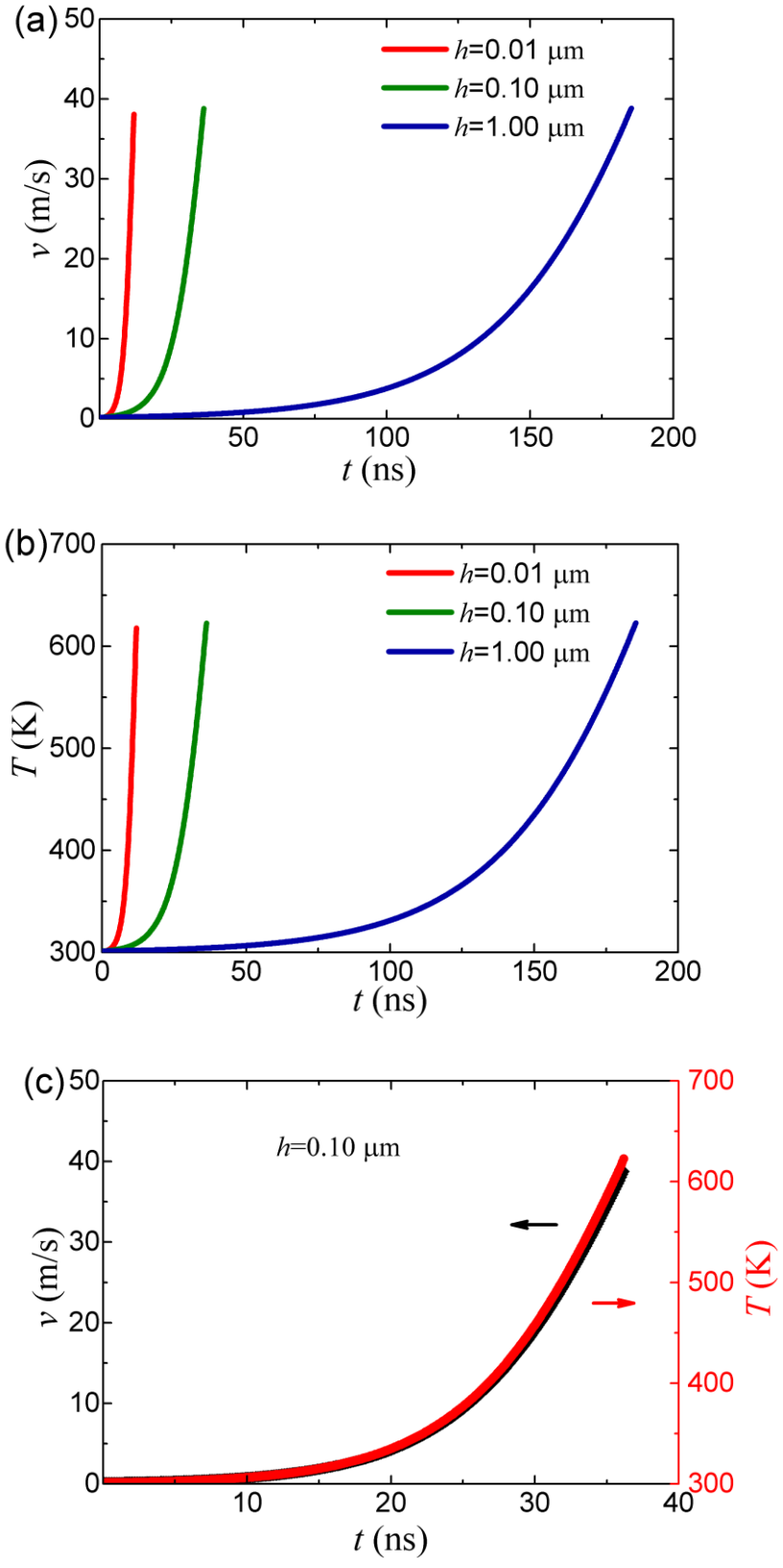

Figure 2 J. G. Wang *et al*

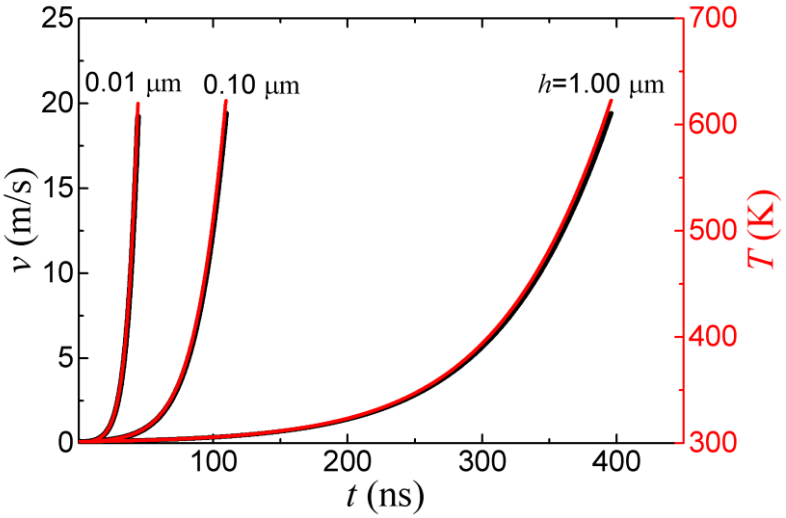

Figure 3 J. G. Wang *et al*

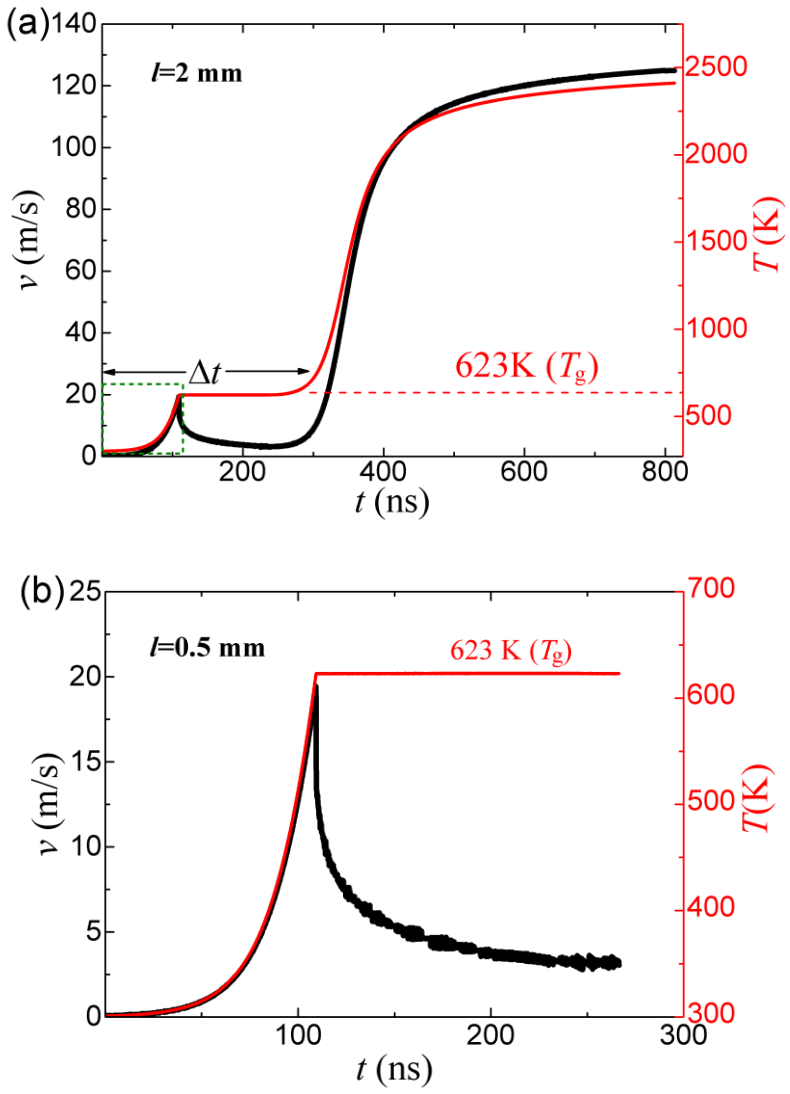

Figure 4 J. G. Wang *et al*

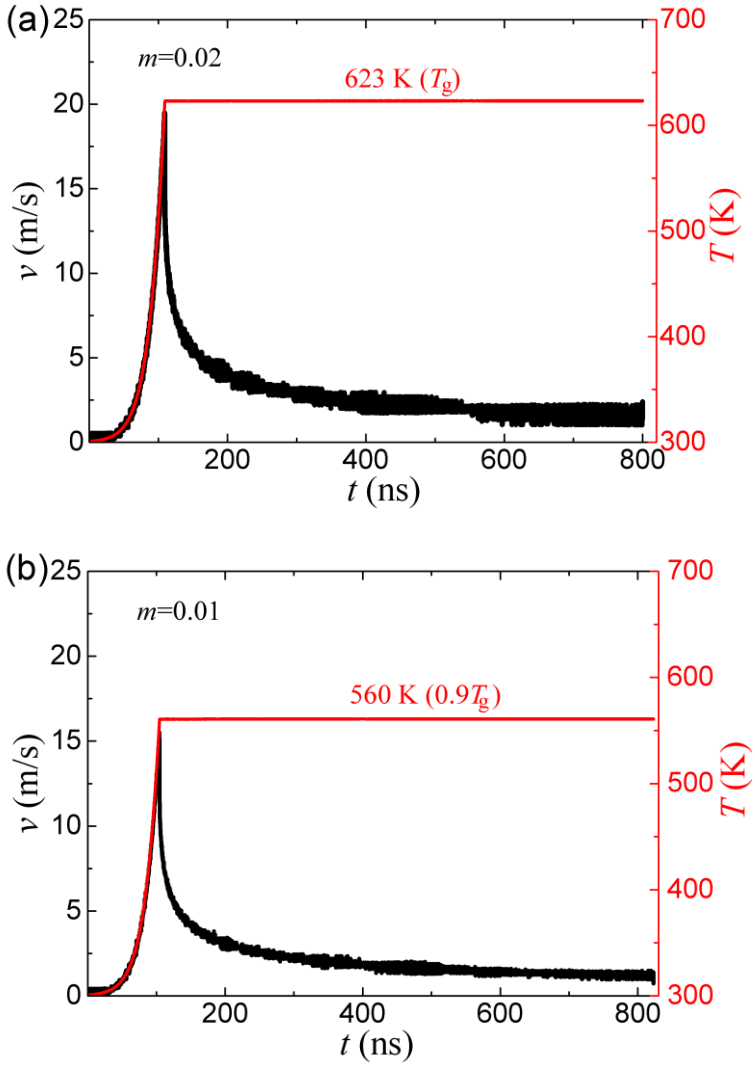

Figure 5 J. G. Wang *et al*

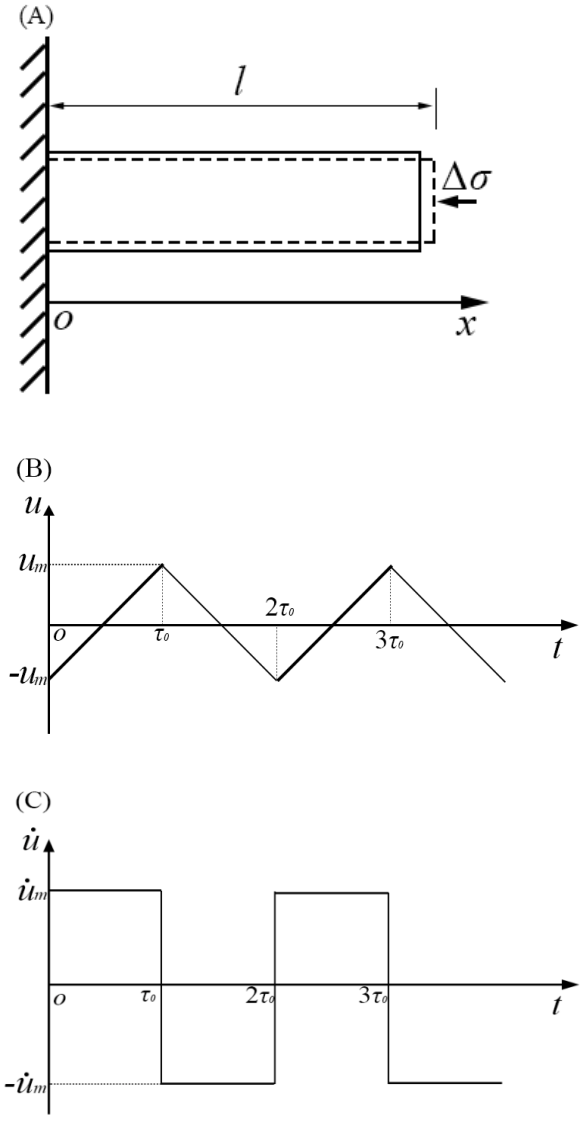

Figure in Appendix J. G. Wang *et al*